

Tailoring Artificial Neural Networks for Optimal Learning

Pau Vilimelis Aceituno^{1,2}, Gang Yan³, Yang-Yu Liu^{1,4}

¹*Channing Division of Network Medicine, Brigham and Women’s Hospital, Harvard Medical School, Boston, Massachusetts 02115, USA*

²*Max Planck Institute for Mathematics in the Sciences, 04103 Leipzig, Germany*

³*School of Physics Science and Engineering, Tongji University, 200092 Shanghai, China*

⁴*Center for Cancer Systems Biology, Dana Farber Cancer Institute, Boston, Massachusetts 02115, USA*

As one of the most important paradigms of recurrent neural networks, the echo state network (ESN) has been applied to a wide range of fields, from robotics to medicine to finance, and language processing. A key feature of the ESN paradigm is its reservoir—a directed and weighted network—that represents the connections between neurons and projects the input signals into a high dimensional space. Despite extensive studies, the impact of the reservoir network on the ESN performance remains unclear. Here we systematically address this fundamental question. Through spectral analysis of the reservoir network we reveal a key factor that largely determines the ESN memory capacity and hence affects its performance. Moreover, we find that adding short loops to the reservoir network can tailor ESN for specific tasks and optimal learning. We validate our findings by applying ESN to forecast both synthetic and real benchmark time series. Our results provide a new way to design task-specific recurrent neural networks, as well as new insights in understanding complex networked systems.

arXiv:1707.02469v1 [cs.LG] 8 Jul 2017

Introduction

Echo state network (ESN) is a promising paradigm of recurrent neural networks that can be used to model and predict the temporal behavior of nonlinear dynamic systems ¹. As a special form of recurrent neural networks, ESN has feedback loops in the randomly assigned and fixed synaptic connections and trains only a linear combination of the neurons' states. This fundamentally differs from the traditional feed-forward neural networks, which have multiple layers but no cycles ² and surpasses other recurrent neural network architectures that suffer from the difficulty in training synaptic connections ³. Owing to its simplicity, flexibility and empirical success, ESN and its variants have attracted intense interest during the last decade ^{4,5}, and have been applied to many different tasks such as electric load forecasting⁶, robotic control⁷, epilepsy forecasting⁸, stock price prediction⁹, grammar processing ¹⁰, and many others ^{6,11-13}.

An ESN can be viewed as a dynamic system from which the information of input signals is extracted ¹⁴. It has been shown that the information processing capacity of a dynamic system in theory depends only on the number of linearly independent variables or, in our case, neurons ¹⁴⁻¹⁶. Yet, the theoretical capacity does not imply that all implementations are practical ^{17,18}, nor does it mean that any reservoir is equally desirable for a given task. A clear example is the effect of the reservoir's spectral radius (i.e., the largest eigenvalue in modulus): an ESN with a larger spectral radius has longer-lasting memory, indicating that it can better process information from past inputs ⁵.

This prompts us to address a fundamental question: Given a certain number of neurons,

how does the reservoir network affect the performance of an ESN? While some previous studies attempted to optimize the reservoir by altering its topology^{19–21}, their approaches need to finetune a large number of parameters and the time complexity of generating a good instance is high. Here we systematically address this question, finding that a spectrum-based metric of the reservoir network largely determines the memory capacity of ESN. Our results allow us to easily assess the memory capacity of a particular reservoir network and reveal previously unexplored optimization strategies. Moreover, we show that adding short loops to the reservoir network can adapt ESN for specific tasks, and provide a method for doing so. In turn, the results provide insights into the memory capacity of dynamic systems, offering potential improvements to other types of artificial neural networks.

The ESN Framework

The basic ESN architecture is depicted in Fig. 1. With different coefficients (weights), the input signal and the predicted output from the previous time step are sent to all neurons in the reservoir. The output is calculated as a linear combination of the neuron states and the input. At each time step, each neuron updates its state according to the current input it receives, the output prediction and its neighboring neurons’ states from the previous time step. Formally, the discrete-time dynamics of an ESN with N neurons, one input and one output is governed by

$$\mathbf{x}(t) = f(\mathbf{W}\mathbf{x}(t-1) + \mathbf{w}_{\text{in}}u(t) + \mathbf{w}_{\text{ofb}}y(t-1)), \quad (1)$$

$$y(t) = \mathbf{w}_{\text{out}} \begin{pmatrix} \mathbf{x}(t) \\ u(t) \end{pmatrix}, \quad (2)$$

where $\mathbf{x}(t) = [x_1(t), x_2(t), \dots, x_N(t)]^\top \in \mathbb{R}^N$ denotes the state of the N neurons at time t , $u(t) \in \mathbb{R}$ is the input signal, the vector $\begin{pmatrix} \mathbf{x}(t) \\ u(t) \end{pmatrix} \in \mathbb{R}^{N+1}$ represents the concatenation of $\mathbf{x}(t)$ and $u(t)$, and $y(t) \in \mathbb{R}$ is the output at time t . There are various possibilities for the nonlinear function f , the most common ones being the logistic sigmoid and the hyperbolic tangent². Without loss of generality we choose the latter in this work. The matrix $\mathbf{W} \in \mathbb{R}^{N \times N}$ is the weighted adjacency matrix of the reservoir network describing the fixed wiring diagram of N neurons in the reservoir. There is a rich literature on the conditions that the matrix \mathbf{W} must fulfill^{22–25}. Here we adopt a conservative and simple condition that the reservoir must be a stable dynamic system. The vector $\mathbf{w}_{\text{in}} \in \mathbb{R}^N$ captures the fixed weights of the input connections, which we draw from a uniform distribution in the interval $[-1, 1]$. The vector $\mathbf{w}_{\text{ofb}} \in \mathbb{R}^N$ denotes the fixed weights of the feedback connections from the output to the N neurons, which can induce instabilities if chosen carelessly and may be zero in some tasks⁵. Finally, the row vector $\mathbf{w}_{\text{out}} \in \mathbb{R}^{1 \times (N+1)}$ represents the trainable weights of the readout connections from the N neurons and the input to the output.

A key feature of ESN is that \mathbf{W} , \mathbf{w}_{in} and \mathbf{w}_{ofb} are all predetermined before the training process, and only the weights of the readout connections \mathbf{w}_{out} are modified to $\mathbf{w}_{\text{out}}^*$ during the training process:

$$\mathbf{w}_{\text{out}}^* = \arg \min_{\mathbf{w}_{\text{out}}} \sum_{t=t_0}^{t_0+T} (y(t) - \hat{y}(t))^2, \quad (3)$$

where t_0 is the starting time, T is the interval of the training, and $\hat{y}(t)$ is the target output obtained from the training data. In other words, $\mathbf{w}_{\text{out}}^*$ is the linear regression weights of the desired output $\hat{y}(t)$ on the extended state vector $\begin{pmatrix} \mathbf{x}(t) \\ u(t) \end{pmatrix}$, which can be easily solved⁵. Hence, $\mathbf{w}_{\text{out}}^*$ captures the

underlying mechanism of the dynamic system that produces the training data. Indeed, the right choice of $\mathbf{w}_{\text{out}}^*$ can be used to forecast, reconstruct or filter nonlinear time series.

To be consistent with the previous literature¹²⁶, and to ease the comparison with other approaches, here we focus on a typical task of ESN, i.e., forecasting time series. We employ the classical Mackey-Glass model to generate synthetic benchmark time series²⁷. We also use two real benchmark time series datasets^{28,29}. To quantify the performance of an ESN, we calculate the normalized root mean square error^{1,26,30}:

$$\sigma = \sqrt{\frac{\sum_{t=t_0}^{t_0+T} (y(t) - \hat{y}(t))^2}{T \cdot \text{var}(u(t))}}, \quad (4)$$

where the target output $\hat{y}(t)$ is predicted for T time steps¹, and $\text{var}(u(t))$ represents the variance of the original signal (see Methods: Performance Measurement for details).

Results

The impact of network properties

Over the past two decades we have witnessed many advances in network science, especially the understanding of how significantly the network structure affects various network functions and dynamical processes, from error and attack tolerance^{31,32} to epidemic spreading^{33,34}, interdependent fragility,³⁵ and controllability³⁶. It is fairly reasonable to expect that the structure of the reservoir network, encoded by the matrix \mathbf{W} , would affect the performance of the corresponding ESN as well.

We first study the impact of degree heterogeneity of the reservoir network on the ESN per-

formance in forecasting the Mackey-Glass time series⁴ (see Methods: Forecasting Mackey-Glass time series). To achieve that, we construct scale-free (SF) reservoir networks with power-law degree distributions $p(k) \sim k^{-\gamma}$ ($\gamma > 2$)³⁷, with a smaller γ meaning a more heterogeneous degree distribution. The edge weights are drawn from a normal distribution with zero mean and a variance implicitly determined by the number of edges, network size and spectral radius. Consistently with previous studies³⁸, we find that the prediction error σ decreases when γ increases (Fig. 2a), indicating that the degree heterogeneity of reservoir networks is detrimental to the ESN performance. Similarly, increasing the average degree $\langle k \rangle$ seems to improve ESN performance for SF networks to some extent. By contrast, the average degree for Erdős-Rényi (ER) random graphs or random regular (RR) graphs does not have any significant effect on the ESN performance (Fig. 2b).

We then investigate the impact of the edge weight distribution, finding that the use of normal, uniform or binary distributions does not affect the ESN performance. Yet, when the absolute value of the edge weights are drawn from a power-law distribution $p(|w|) \sim |w|^{-\beta}$ ($\beta > 0$), we find that across all studied topologies, the larger the β , the better the performance (Fig. 2c).

Our results in Fig. 2 suggest that there are several parameters that can affect the ESN performance. Moreover, the same parameter may have disparate effects in different types of networks, making the search for an optimal reservoir rather challenging.

The driving factor determining ESN memory

The success of ESN in tasks such as forecasting time-series comes from the ability of its reservoir in retaining memory of previous inputs. It has been shown that some reservoir architectures re-

quire different spectral radius to retain the same amount of memory³⁹. Thus, to reveal the driving factor that determines the ESN performance, we first explore how the reservoir network affects the memory capacity of ESN.

The following measure has been proposed to quantify the memory capacity of a reservoir⁴⁰:

$$M = \sum_{\tau=1}^{\tau_{\max}} M_{\tau}, \quad (5)$$

with $M_{\tau} = \max_{\mathbf{w}_{\text{out}}^{\tau}} \frac{\text{cov}^2(r(t-\tau), y_{\tau}(t))}{\text{var}(r(t-\tau))\text{var}(y_{\tau}(t))}$. Here $r(t)$ is a random variable drawn from a uniform distribution $\mathcal{U}(-1, 1)$, serving as a random input, 'cov' represents the covariance, $y_{\tau}(t)$ is the output as described in Eq. 1, $\mathbf{w}_{\text{out}}^{\tau}$ is chosen to minimize the difference between $y_{\tau}(t)$ and $r(t-\tau)$ for any delay $\tau \in [1, \dots, \tau_{\max}]$, with τ_{\max} chosen so that $M_{\tau_{\max}} \approx 0$.

While the memory capacity M does correlate with the parameters β , γ , and $\langle k \rangle$ that affect ESN performance, by itself it is not very useful for our purpose. Indeed, considering the reservoir as a black box that simply generates values, this metric M fails to explain why β and γ affect the memory, while other parameters like $\langle k \rangle$ in ER or RR graphs do not. Furthermore, it is of little practical interest, since obtaining M requires much more computational power than training and testing one ESN instance.

To better quantify the relationship between the reservoir dynamics and the memory capacity, we note that the extraction of information from the reservoir is made through a linear combination of the neurons' states. Hence it is reasonable to assume that more linearly independent neurons would offer more variable states, and thus longer memory^{41,42}. In plain words, we hypothesize that

the memory capacity M strongly depends on the correlations among neuron states, which can be quantified as follows:

$$S = \frac{2 \sum_{i=1}^{N-1} \sum_{j=i+1}^N P_{ij}^2}{N(N-1)}. \quad (6)$$

Here $P_{ij} = \frac{\text{cov}(x_i(t), x_j(t))}{\text{std}(x_i(t))\text{std}(x_j(t))}$ is the Pearson's correlation coefficient between the states of neurons i and j , and $\text{std}(x_i)$ represents the standard deviation. Note that S is simply the average of those squared correlation coefficients, representing a global indicator of the correlations among neurons in the reservoir. Fig. 3a corroborates our hypothesis, showing that for all topologies there is a strong correlation between S and M . Thus, hereafter we only need to understand how the network structure affects the neuron correlation.

We consider the neuron correlation as a measure of coordination. If the neuron states are highly interdependent, then S will be very high. By contrast, a system with independent neurons will have very low S . Qualitatively, this explains the impact of degree heterogeneity on the ESN performance, since in degree heterogeneous networks the states of many nodes will heavily depend on the states of the hubs (nodes with high degrees), thus increasing their overall correlations. For linear dynamical systems, the correlations between neurons can be quantified through the eigenvalues of the adjacency matrix. Our system is non-linear, but given the specific type of nonlinearity in the hyperbolic tangent function $f(z) = (e^z - e^{-z})/(e^z + e^{-z})$, we can relate the correlations with the linearization of $f(z)$ around $z = 0$, which is nothing but the identity function $f(x) = x$. Hence we can use the eigenvalues of matrix \mathbf{W} to approximately quantify how fast the input decays in the reservoir, and hence how poorly the ESN remembers. This is further supported by two facts (1) the spectral radius affects the memory of the reservoir⁴³; (2) networks showing lower correlation

among neuron states have eigenvalues almost uniformly distributed in the complex plane, while networks with higher correlations tend to have more eigenvalues concentrated around zero with lower moduli.

To quantify the aggregated effect of the eigenvalue distribution in the complex plane, we define the average eigenvalue moduli:

$$\langle |\lambda| \rangle = \frac{\sum_{i=1}^N |\lambda_i|}{N}, \quad (7)$$

where λ_i 's are the eigenvalues of the matrix \mathbf{W} . As expected from our previous discussion, we find that $\langle |\lambda| \rangle$ strongly correlates with S (see Fig. 3b). The correlation of $\langle |\lambda| \rangle$ with S and therefore with M indicate that $\langle |\lambda| \rangle$ indeed reflects the memory capacity of the reservoir. As opposed to M and S , $\langle |\lambda| \rangle$ is much easier to compute and is solely determined by the reservoir network. This offers us a very simple network measure to quantify the ESN memory capacity.

To demonstrate the meaning of $\langle |\lambda| \rangle$ in studying ESN performance, we applied ESN to forecast the classical Mackey-Glass time series, the Laser Intensity time series^{28,44} obtained from the Santa Fe time series Competition Data, and the recognition of the Spoken Arabic Digit Data Set²⁹ downloaded from the UCI Machine Learning Repository⁴⁵, see Fig. 4 and Methods. We present the ESN performance of those three tasks in Fig. 5. We find that for each task there is a small range of $\langle |\lambda| \rangle$ that achieves the best performance across various network topologies, suggesting the existence of a specific memory capacity required for each task.

Adapting ESN to a specific frequency band

Besides the memory capacity, there are other features that are relevant for machine learning tasks. A key factor in time-series processing and dynamic systems modeling is the frequency spectrum^{46–48}. Any signal or time series can be expressed in terms of its spectrum, which reflects the decomposition of signals into sinusoids with different frequencies⁴⁹. This type of characterization usually offers valuable insights into the nature or underlying dynamics of the system, and has been exploited for various applications⁵⁰.

In the context of ESN, we can prove that the performance for a given task is bounded by the dissimilarity between the power spectral density (PSD) of the reservoir and that of the target variable $y(t)$. Intuitively, this means that if we create a linear projection from the state of the reservoir to the target variable, this projection will be more robust and precise if the neural states are already very similar to the target variable. Since one of the most common and powerful approaches to quantifying similarities of time-series data is through the PSD⁵¹, it is natural to use it in our context.

Knowing that altering the reservoir’s PSD may increase the ESN’s performance, we must now create reservoirs with specific frequency bands. Our approach is a simple extension of classical Infinite Impulse Response filters from Signal Processing⁵⁰: we add feedback loops with delay L in our neurons, encoded as cycles of length L in the network. We account for the number and strength of those cycles by using the following variable:

$$\rho_L = \frac{\mathbb{E}[(\mathbf{W}^L)_{ii}]}{\mathbb{E}[|(\mathbf{W}_{ij})^L|]}, \quad (8)$$

where \mathbb{E} is the expectation operator. Note that in the classical ESN, any cycle has equal probability

of providing positive or negative feedback, rendering $\rho_L = 0$ for any $L > 0$. We prove that ρ_L can be used to tune the average PSD of the reservoir with random input. Specifically, by adding cycles of a desired length into the reservoir and hence increasing ρ_L (see Methods), we can tune the response of the reservoir’s average neuron state to specific frequencies, as shown in the colored lines in Fig. 6. This behavior has a natural visualization in terms of the eigenvalues of the adjacency matrix, which change with ρ_L .

We show in Fig. 7 that the performance of ESN can indeed be substantially improved by adding certain short loops to the reservoir to enhance or dampen specific frequency bands. A simple example is given by the Mackey-Glass time series: The plots in Fig. 6 show that for $\rho_L > 0$, the reservoir’s average PSD response is enhanced for the frequencies close to 0, which is the area where the spectrum of the Mackey-Glass Time Series is concentrated. Consistent with our hypothesis, this improves the ESN performance on forecasting the Mackey-Glass Time Series (see Fig. 7.a, d, g), because the average PSD response of the reservoir matches the PSD of the Mackey-Glass Time Series. Similarly, the Spoken Arabic Digits are also dominated by frequencies close to 0, and thus the performance of ESN improves when $\rho > 0$ (see Fig. 7c,f,i). As for the Laser Intensity Time Series, its dominating frequencies are around 0.13, 0.27 and 0.38, thus ESN is improved when the response of the reservoir enhances those frequencies. As shown in Fig. 6.e,h, this happens when $\rho_L < 0$ for $L = 2, 3$. For the case of $L = 1$, we observed in Fig. 6.b that the three peaks cannot be all enhanced simultaneously by setting ρ_1 to be either positive or negative, so we expect $\rho_1 \approx 0$.

Those results strongly suggest that the reservoir should enhance the frequencies present in the target signal. A simple way of achieving that result is to obtain the frequency responses of the reservoir for an unstructured signal (white Gaussian noise), and then select the parameters of the reservoir for which the frequencies match the target signal better. An algorithm designed based on those considerations is presented in the Methods section.

Altering the PSD by adding cycles changes the distribution of eigenvalues, specifically creating some extreme values that are larger than in the original, non-adapted adjacency matrix. This obviously affects the spectral radius, but not $\langle |\lambda| \rangle$. Since we expect that the memory requirement for a task is not affected by adapting the PSD, it is reasonable to use $\langle |\lambda| \rangle$ as the normalization variable for the weights of reservoir matrix, instead of the spectral radius. We can thus use the optimal value of $\langle |\lambda| \rangle$ found by in classical ESN before adapting the PSD.

The results presented in Fig. 7 show that our simple algorithm does increase ESN performance beyond what can be achieved with classical ER reservoirs with $\rho = 0$.

Discussion

In this paper we explore how simple ideas from classical signal processing and network theory can be applied to tailor ESN for optimal learning. We find that the memory capacity depends on the distribution of all the eigenvalues of the connectivity matrix \mathbf{W} , a result that goes beyond current ESN practice and theory, where the main memory parameter is the spectral radius. Moreover, we demonstrate that ESN practitioners should consider the frequency of the time series that they process, and provide simple tools to tune reservoirs to a specific frequency.

We expect that the results presented here will help engineers and scientists better adapt the ESN memory and working frequency for specific tasks. A straightforward extension would be to provide a more advanced network generation algorithms which incorporate general motifs instead of cycles, thus creating more accurate frequency responses in the reservoir.

We believe the presented results have implications in solving other related machine learning problems. Other recurrent neural networks can be improved by using our results, either through selection of appropriate initial topologies in a pre-training stage, or by designing learning algorithms that account for the principles outlined here. Given that most current learning strategies such as backpropagation focus on adapting single weights, we are convinced that many new learning algorithms can be created based on the adaptation of network motifs and macroscopic network parameters such as degree heterogeneity.

Acknowledgments

We would like to thank Professor Jäger from the Jacobs University for his invaluable advice and technical help. We also are grateful to Dr. Benjamin Liebald for sharing his code and data with us. This work was partially supported by the John Templeton Foundation (Award No. 51977), and the “Fundaci Bancaria la Caixa” who funded Mr. Pau Vilimelis Aceituno through its fellowship program.

Author Contributions. Y.-Y.L. conceived and designed the project. P.V.A. performed all the analytical calculations and empirical data analysis. P.V.A. and G.Y. performed extensive numerical simulations. All authors analyzed the results. P.V.A. and Y.-Y.L. wrote the manuscript. G.Y. edited the manuscript.

Competing Interests. The authors declare that they have no competing financial interests.

Correspondence. Correspondence and requests for materials should be addressed to Y.-Y.L. (yy1@channing.harvard.edu).

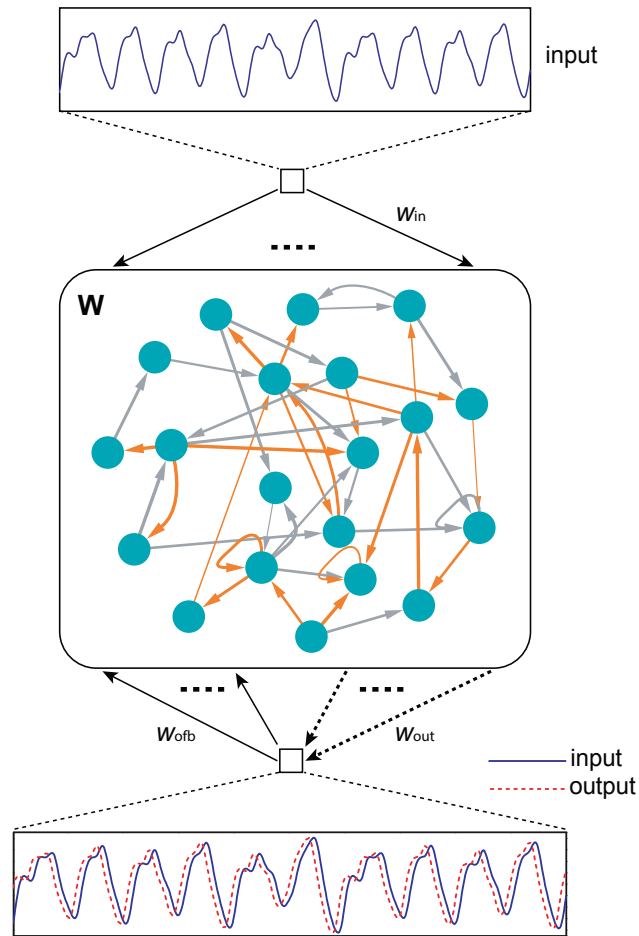


Figure 1 The basic schema of an ESN. The input signal $u(t)$ goes to each neuron in the reservoir with input weights w_{in} , the neurons send their states to their neighbors according to the matrix \mathbf{W} , and the contribution of each neuron to the output $y(t)$ is collected by w_{out} . During the training period, the difference between the output $y(t)$ and the input $u(t)$ is sent back to the reservoir with the weights w_{ofb} . The reservoir network may have self-loops, and can have both excitatory (yellow) and inhibitory (gray) synaptic connections.

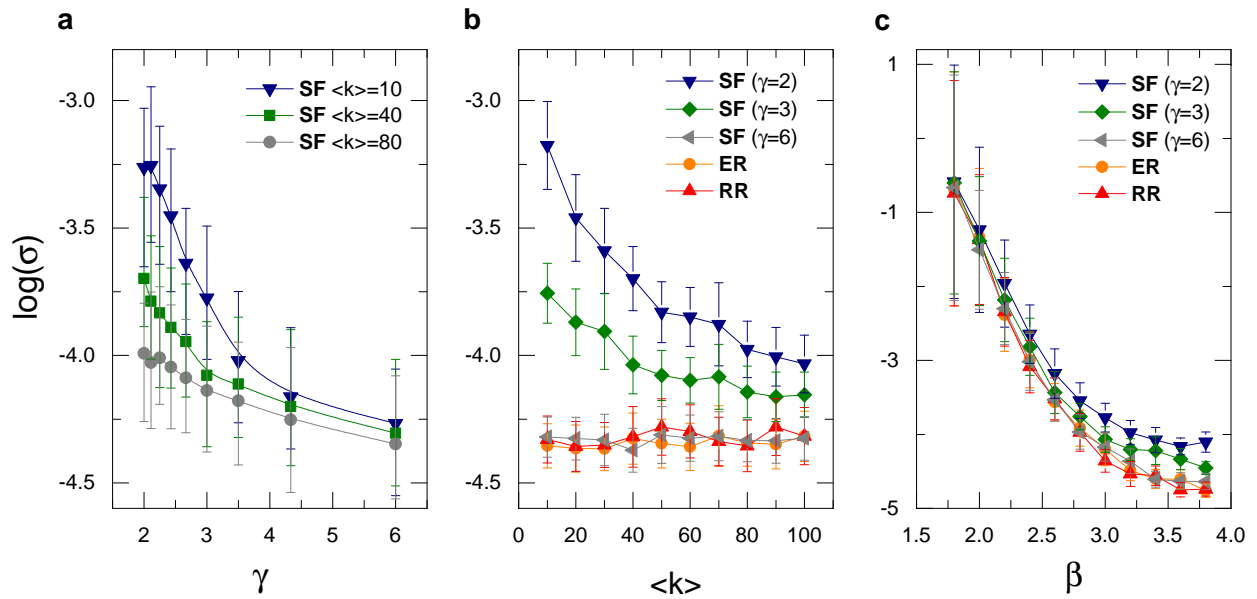


Figure 2 Impacts of various network properties on the ESN performance. (a) The prediction error σ as a function of the exponent γ of the power-law degree distribution for scale-free (SF) networks. As γ increases the neurons' degrees become more homogeneous. (b) σ vs. average degree $\langle k \rangle$ for random regular (RR) graphs, SF networks, and Erdős-Rényi (ER) random graphs. (c) σ as a function of the exponent β of the power-law link weight distributions. As β increases the link weights become more homogeneous.

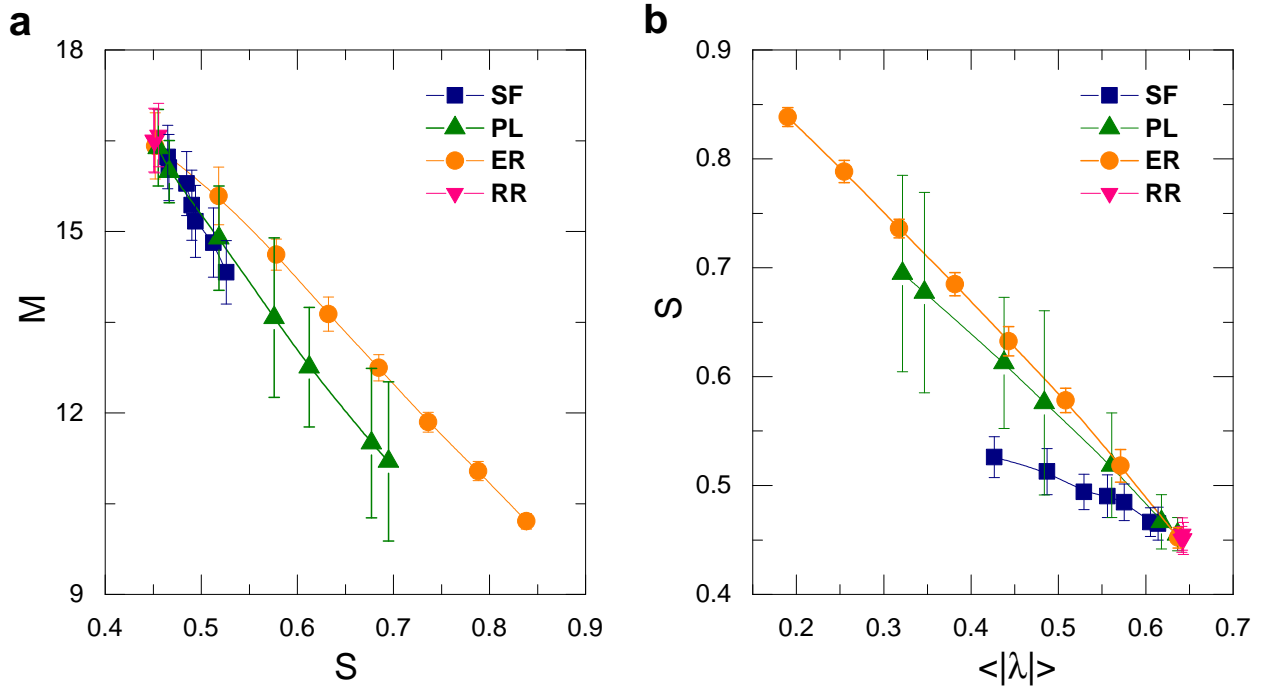


Figure 3 Relationship between memory capacity, neuron correlation and the network spectrum. (a) Memory capacity M vs neuron state correlation S . (b) Neuron state correlation S vs average eigenvalue modulus $\langle |\lambda| \rangle$. The ESNs were created using reservoirs of 400 neurons with spectral radius of 1 and sequences of 4000 random inputs uniformly distributed in the interval $[-1, 1]$. The SF curve corresponds to scale-free networks with tunable exponent γ , with lower γ corresponding to lower M , higher S and lower $\langle \lambda \rangle$. The PL values are for Erdős-Rényi random graphs with weights drawn from a PL distribution with varying β , and the points with lower β have lower M , higher S and lower $\langle \lambda \rangle$. All networks have a spectral radius $\alpha = 1$, except the ER networks where each point corresponds to a spectral radius increasing from 0.2 to 1. The ER networks are plotted with various spectral radius to show the effects of that parameter. Since ER

networks correspond to the limit cases of both RR and SF networks, the curves for ER networks also indicate how would RR and SF networks behave if their spectral radius are changed.

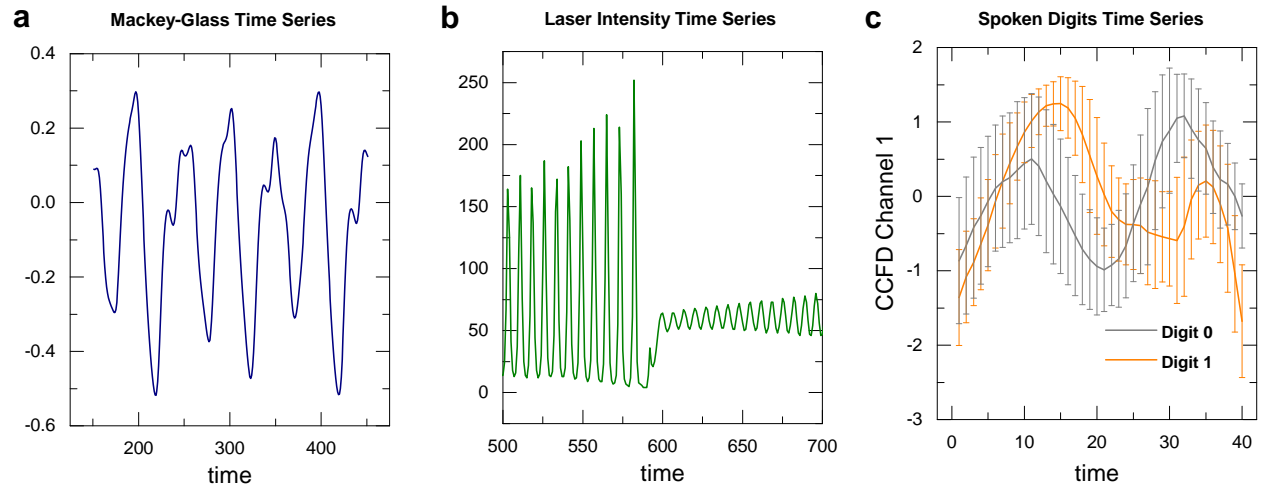


Figure 4 Benchmark time series data analyzed in this paper. (a) the Mackey-Glass time series with 500 points. (b) the Laser Intensity time series with 300 points. (c) the average value of the first CCFD Channel with the standard deviation for 330 recordings. See the Methods sections for an expanded description of the three datasets.

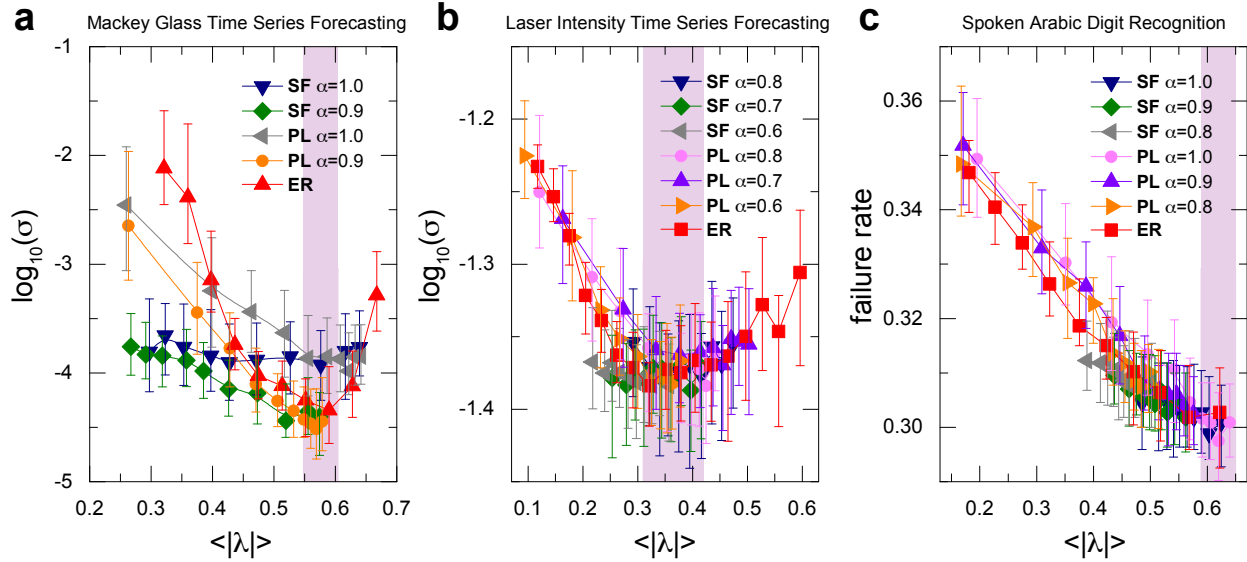


Figure 5 ESN performance explained by $\langle |\lambda| \rangle$. The performance of ESN as a function of the average eigenvalue modulus $\langle |\lambda| \rangle$ for three tasks: (a) Mackey Glass time series forecasting, (b) laser intensity time series forecasting, and (c) spoken Arabic digit recognition. For each task, we use scale-free networks (SF), Erdős-Rényi networks with homogeneous link weights (ER), and Erdős-Rényi networks whose link weights follow a power-law distribution (PL) as reservoirs. The SF and PL networks have various spectral radii α , chosen to be around the optimal value of α for the Erdős-Rényi case. The three panels show that, regardless of topology or spectral radius, all networks have their optimal performance when the average eigenvalue module, $\langle |\lambda| \rangle$, is within the intervals $[0.55, 0.6]$ (a), $[0.3, 0.4]$ (b), or $[0.6, 0.7]$ (c), which are highlighted in gray. Since the value of $\langle |\lambda| \rangle$ is correlated with the memory capacity, and the presented tasks have specific memory requirements, the results are consistent with our discussion in the main text.

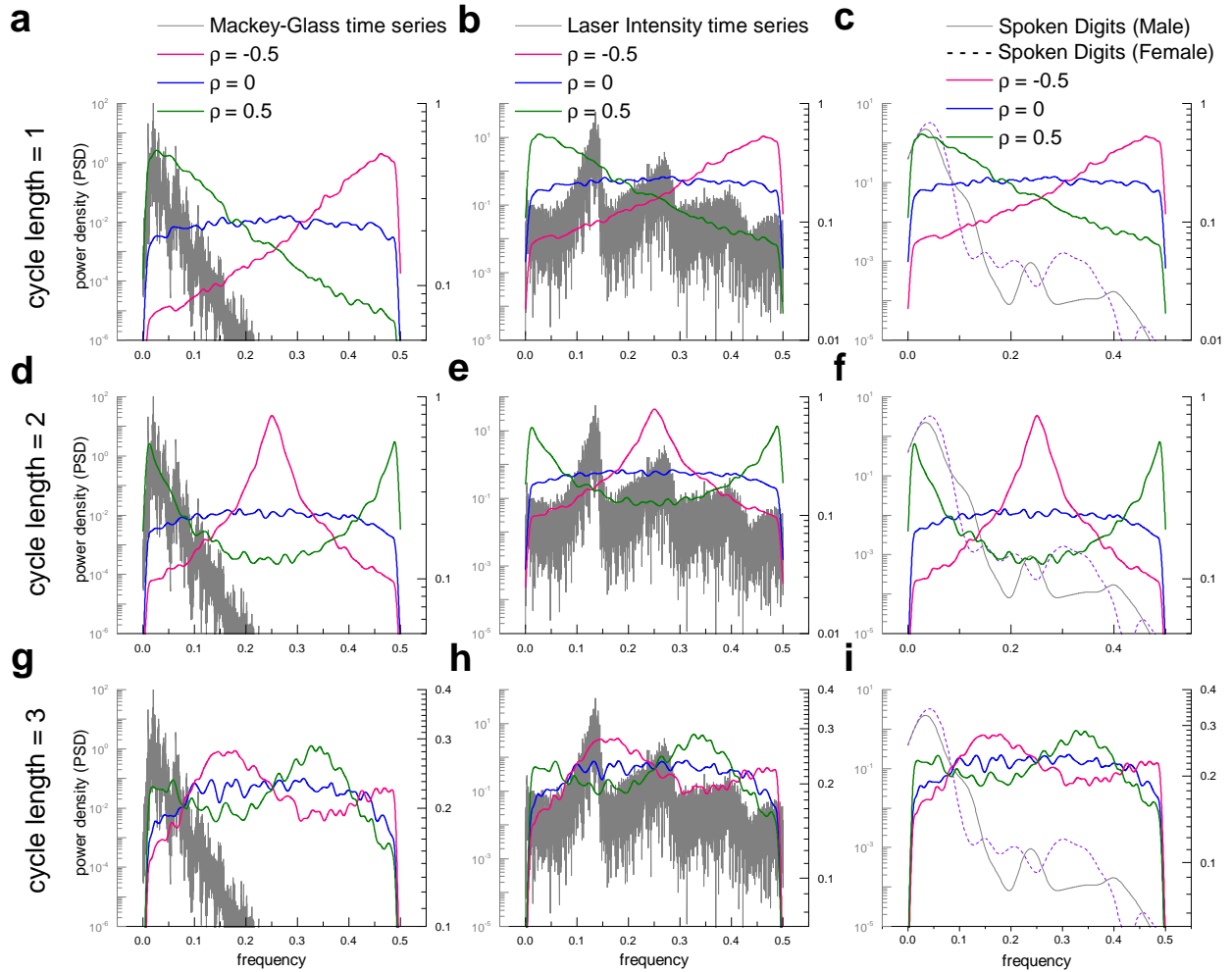


Figure 6 Frequency domain analysis of target signals and reservoir frequencies.

We plotted the power spectral density (PSD) of three empirical time series (Mackey-Glass in a, d, g; Laser Intensity in b, e, h; Spoken Digits in c, f, i), and the average PSD of the reservoirs' neuron states for reservoirs with various ρ when using a random Gaussian input with zero mean and variance of one (left y-axis for PSD of empirical time series and right y-axis for PSD of reservoirs with random inputs). In each panel we plot the average PSD of 500 reservoirs with 400 neurons and connectivity 0.05 (see Methods:

Generating Networks with ρ_L). The length of cycles added into the reservoir is 1 (a-c), 2 (d-f) and 3 (g-i). Note that changing the reservoir through adding cycles can make the response of neurons similar to the signal's. In the case of Mackey-Glass and Spoken Arabic Digit, the signals have slow variations, and are thus defined mostly by frequencies close to 0. Furthermore, any reservoir with $\rho > 0$ will enhance the frequencies close to 0, meaning that such a reservoir would enhance the frequencies relevant to those two signals. Similarly, the Laser Intensity has three peaks that are closer to the center of the spectrum, which are enhanced in the cases of $\rho < 0$ for $L = 2$ and $L = 3$, but not for $L = 1$, in which case neither $\rho > 0$ nor $\rho < 0$ will enhance the three peaks. This will have important implications on the performance of ESN (see Fig. 7).

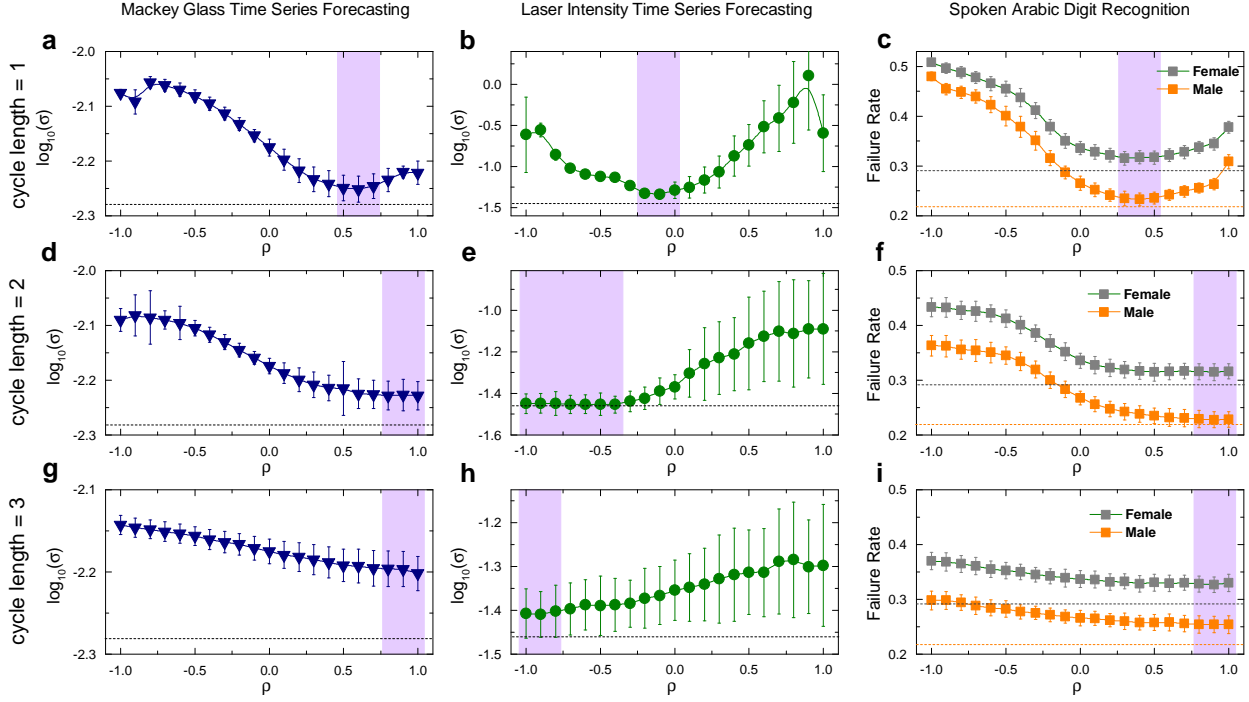


Figure 7 Improving ESN through frequency adaptation. ESN performance σ vs ρ_L , for the tasks of Mackey-Glass Forecasting (a, d, g), Laser Intensity Forecasting (b, e, h), and Spoken Arabic Digit Recognition (c, f, i). The length of cycles added into the reservoir is 1 in (a-c), 2 in (d-f) and 3 in (g-i). The dashed lines correspond to the performances obtained for each task by creating reservoirs with combinations of cycles of various lengths using the algorithm presented in the Methods section. Following our observation in Fig. 6, the performance of ESN increases when the the reservoir enhances the frequencies that are dominant in the signal. Thus, since the Mackey-Glass and Spoken Arabic Digit signals have low frequencies, the performance of ESN for those signals increases when $\rho > 0$. In contrast, the Laser Intensity time series is defined by frequencies that are on the center of the spectrum, thus ESN has a better performance when $\rho_1 \simeq 0$, $\rho_2 < 0$ and

$\rho_3 < 0$, as those parameters adapt the reservoir's response to the time-series frequencies. In all cases we see that combining cycles of different lengths can bring substantial improvements to ESN performance.

Methods

Performance Measurement

Figures 2, 5, 6 measure the performance of ESN for different parameters and network structures. In each case we used 200 network samples per parameters. Each of those experiments gives a certain performance described in the following paragraphs.

In the literature of ESN it is common to use the normalized root mean squared error (NRMSE), as a metric for an error. This metric is a normalization of the classical root mean squared error (RMSE). The normalization is necessary in this case to avoid having different values if the signal is multiplied by a scalar. This is particularly important in ESN because one of the parameters that is usually tuned⁵ is the scaling of the input vector w_{in} or the input signal $u(t)$. If the error metric was not normalized, then the scaling would always be low. The parameter t_0 is used to describe where the network should start to count the performance, since it is also common to ignore the inputs during the initialization phase⁵, which is taken here as the full initialization steps given for each task (see details in the subsequent sections). The parameter T is simply the number of time-steps considered, which we take here as the full count of all points (minus the initialization) in each testing time series.

The NRMSE is obviously not a significant metric for classification, since the target variable is a boolean. In order to have a comparable metric for the performance, we use the failure rate in classification. Note that having 10 digits implies that the failure rate with random guesses is 0.9, therefore a failure rate of 0.3 is well below it.

When designing an ESN implementation, the classical approach is to try many reservoirs and take the one that gives the best performance. It is therefore natural not to account for outliers with low performances, since they will never be picked. Conversely, taking only the best performance gives noisy results that require a computationally prohibitive amount of computations. Thus, in the figures presented here we plot the median as the central point and upper and lower quartile as error bar.

Forecasting Mackey-Glass time series

Forecasting Mackey-Glass time series is a benchmark task of ESN ¹. The Mackey-Glass time series follows the ordinary differential equation:

$$\frac{ds}{dt} = \beta \frac{s_\tau}{1 + s_\tau^n} - \gamma s,$$

where β, γ, τ, n are real positive numbers, and s_τ represents the value of the variable s at time $t - \tau$. We used the parameters $\beta = 0.2, \gamma = 0.1, \tau = 17, n = 10$ in our simulations. The discrete version of the equation uses a time step of length $h = 0.1$. For each instance we initialized the time series with $\frac{\tau}{h} = 170$ uniformly distributed random values between 1.1 and 1.3, then the first 1000 points were considered initialization steps which did not fully capture the time series dynamics and were thus discarded. For Fig. 2 and 5 the prediction was done using an ESN with a reservoir of 1000 neurons as done in ¹, average degree $\langle k \rangle = 50$, which is different from ¹ but more convenient for studying networks. In Fig. 2, we used the spectral radius $\alpha = 0.85$, which is the one used in ¹. We used 1000 points for initialization and 9000 for training, then we computed a new time series and used the first 1000 points for initialization and 9000 for testing. For Fig. 7, the quality and abundance of data made the use of cycles irrelevant. In order to show the interest

of our contribution, we normalized the signal to have mean zero and variance of one and we added Gaussian white noise with $\sigma = 0.05$, and the forecasting was done using reservoirs of 100 neurons, average degree $\langle k \rangle = 10$ and spectral radius of $\alpha = 0.85$, without feedback so $w_{\text{ofb}} = 0$.

Forecasting Laser Intensity time series

The second task consist on forecasting the Laser Intensity time series^{28,44} obtained from the Santa Fe Institute time series Forecasting Competition Data. It consists of 10093 points, which we normalized to have an average of 0 and an standard deviation of 1, and filtered with a Gaussian window of length 3. The forecasting was done using reservoirs of 100 neurons, average degree $\langle k \rangle = 10$ and spectral radius of $\alpha = 0.9$, without feedback so $w_{\text{ofb}} = 0$. We used 1000 points of the time series used for initialization, 4547 for training and 4546 for testing. Note that in this case the starting reservoir state for the testing phase was the same as the last reservoir state during the training phase.

Spoken Arabic Digit Recognition

We used ESN for the task of recognizing Spoken Arabic Digits²⁹ with dataset obtained from the Spoken Arabic Digit Data Set²⁹ from the UCI Machine Learning Repository⁴⁵. This dataset consists of 330 recordings for each of the ten digits and two sexes for training, and 110 recordings for testing. Each recording was a time series of varying length encoded with MCCF⁵² with 13 channels. While using the three first channels gave a large performance, we use only the first channel, which is akin to a very lossy compression. We normalized this time series to have average of 0 and a standard deviation of 1, and a length of 40, with the values computed through interpolation. The

classification procedure was done using the forecasting framework from before. We collected the reservoir states from all the training examples of each digit and computed the \mathbf{w}_{out} for forecasting as done in the previous cases. In the testing we collected the states and matched the forecasting with the actual data, obtaining a performance value σ for each of the 20 cases. We classified the time series as the digit that yielded the lowest forecasting error. We used reservoirs of 100 neurons, average degree $\langle k \rangle = 10$ and spectral radius of $\alpha = 1$, without feedback so $\mathbf{w}_{\text{ofb}} = 0$, as in our simulations the performance was similar with or without output feedback.

Generating Networks with ρ_L

In order to create networks that meet our needs, we designed an algorithm in which the variable r_L determines the relative influence of a specific frequency by adding cycles of length L , and s is the sign (positive implies enhancement, negative dampening).

If $L = 1$: Create a random sparse matrix W_r with $N(N - 1)c$ entries. Normalize the spectral radius to 1 and then $\mathbf{W} = \alpha((1 - r_1)W + r_1I)$.

Else :

Step-1: Create $\frac{r_L N^2 c}{2L}$ permutations of length $L - 1$ of numbers picked from 1 to N without repetition. Each permutation is a cycle.

Step-2: For each cycle, pick a random value from a Normal distribution with zero mean and a variance of one and assign it to all the edges.

Step-3: For each cycle, if the sign of the product of the edge weights is not the same as s , multiply

the last edge by -1 . This process generates an adjacency matrix W_c .

Step-4: Create a random sparse matrix W with $\frac{(1-r_L)N^2c}{2}$ entries and weights drawn from a Normal distribution with zero mean and a variance of one. Normalize the spectral radius to 1 and then $\mathbf{W} = (W_r + W_c)$.

Step-5: Normalize to the desired spectral radius $\mathbf{W} \leftarrow \frac{\mathbf{W}}{\lambda_M} \alpha$

The special treatment of the case $L = 1$ is due to the fact that with length of 1 if all edges are self loops the network is fully disconnected and the number of edges is at most N , meaning that for some values of ρ_1 the number of edges would be lower than the number required by the connectivity parameter. For a discussion on the relationship between the case where $L = 1$ and leaky integrator neurons.

Note that the variable r_L and $|\rho_L|$ are indeed the same for sparse networks.

Frequency optimization

The process of finding the optimal $\rho = [\rho_1, \rho_2, \dots, \rho_L]$ is described in this section.

Step-1: Obtain the frequency response of the reservoir $\hat{R}(\rho, L)$ various values of ρ for all the L considered. If this is not stored, compute it by generating Gaussian noise with the same variance and mean as the original signal and use it as an input for the reservoir. Then apply the Fast Fourier Transform to the neurons' states and average over all neurons. Repeat for various reservoir instances.

Step-2: Compute the Fourier transform of the input signal and keep the vector of absolute values $\hat{s} = [\hat{s}(0), \hat{s}(2), \dots, \hat{s}(f_S)]$, where f_S is half the sampling frequency.

Step-3: Compute the scalar product $\langle \hat{s}, \hat{R}(\rho_L, L) \rangle$ for all ρ, L , and select the ρ which maximizes it for each L .

Step-4: Test the performance of an ESN with the values of ρ_L found in the previous step. If the performance is lower than in the default case of $\rho_L = 0$, do not optimize with regard to that length.

Step-5: For all values of ρ where the cycle length is allowed and which fill the condition $\|\rho\|_1 \leq 1$, select the one that maximizes $\sum_L \langle \hat{s}, \hat{R}(\rho_L, L) \rangle$.

1. Jaeger, H. & Haas, H. Harnessing nonlinearity: Predicting chaotic systems and saving energy in wireless communication. *Science* **304**, 78–80 (2004).
2. Bishop, C. M. *Pattern Recognition and Machine Learning (Information Science and Statistics)* (Springer-Verlag New York, Inc., Secaucus, NJ, USA, 2006).
3. Pascanu, R., Mikolov, T. & Bengio, Y. On the difficulty of training recurrent neural networks. *International Conference on Machine Learning* **28**, 1310–1318 (2013).
4. Jaeger, H. The echo state approach to analysing and training recurrent neural networks-with an erratum note. *Bonn, Germany: German National Research Center for Information Technology GMD Technical Report* **148**, 34 (2001).
5. Jaeger, H. *Tutorial on training recurrent neural networks, covering BPPT, RTRL, EKF and the "echo state network" approach* (GMD-Forschungszentrum Informationstechnik, 2002).
6. Deihimi, A. & Showkati, H. Application of echo state networks in short-term electric load forecasting. *Energy* **39**, 327–340 (2012).
7. Plöger, P. G., Arghir, A., Günther, T. & Hosseiny, R. Echo state networks for mobile robot modeling and control. In *Robot Soccer World Cup*, 157–168 (Springer, 2003).
8. Buteneers, P., Schrauwen, B., Verstraeten, D. & Stroobandt, D. Real-time epileptic seizure detection on intra-cranial rat data using reservoir computing. In *International Conference on Neural Information Processing*, 56–63 (Springer, 2008).

9. Lin, X., Yang, Z. & Song, Y. Short-term stock price prediction based on echo state networks. *Expert systems with applications* **36**, 7313–7317 (2009).
10. Tong, M. H., Bickett, A. D., Christiansen, E. M. & Cottrell, G. W. Learning grammatical structure with echo state networks. *Neural Networks* **20**, 424–432 (2007).
11. Verplancke, T. *et al.* A novel time series analysis approach for prediction of dialysis in critically ill patients using echo-state networks. *BMC Medical Informatics and Decision Making* **10**, 1 (2010).
12. Newton, M. J. & Smith, L. S. A neurally inspired musical instrument classification system based upon the sound onset. *The Journal of the Acoustical Society of America* **131**, 4785–4798 (2012).
13. Coulibaly, P. Reservoir computing approach to great lakes water level forecasting. *Journal of Hydrology* **381**, 76–88 (2010).
14. Dambre, J., Verstraeten, D., Schrauwen, B. & Massar, S. Information processing capacity of dynamical systems. *Scientific Reports* **2** (2012).
15. Duport, F., Schneider, B., Smerieri, A., Haelterman, M. & Massar, S. All-optical reservoir computing. *Optics Express* **20**, 22783–22795 (2012).
16. Maass, W., Natschläger, T. & Markram, H. Real-time computing without stable states: A new framework for neural computation based on perturbations. *Neural Computation* **14**, 2531–2560 (2002).

17. Whitley, D. & Watson, J. P. Complexity theory and the no free lunch theorem. In *Search Methodologies*, 317–339 (Springer, 2005).
18. Büsing, L., Schrauwen, B. & Legenstein, R. Connectivity, dynamics, and memory in reservoir computing with binary and analog neurons. *Neural Computation* **22**, 1272–1311 (2010).
19. Ferreira, A. A. & Ludermir, T. B. Comparing evolutionary methods for reservoir computing pre-training. In *Neural Networks (IJCNN), The 2011 International Joint Conference on*, 283–290 (IEEE, 2011).
20. Jiang, F., Berry, H. & Schoenauer, M. Supervised and evolutionary learning of echo state networks. In *Parallel Problem Solving from Nature–PPSN X*, 215–224 (Springer, 2008).
21. Deng, Z. & Zhang, Y. Complex systems modeling using scale-free highly-clustered echo state network. In *Neural Networks, 2006. IJCNN'06. International Joint Conference on*, 3128–3135 (IEEE, 2006).
22. Jaeger, H. Discovering multiscale dynamical features with hierarchical echo state networks. *Jacobs University Bremen, Technical Reports* (2007).
23. Yildiz, I. B., Jaeger, H. & Kiebel, S. J. Re-visiting the echo state property. *Neural Networks* **35**, 1–9 (2012).
24. Buehner, M. & Young, P. A tighter bound for the echo state property. *IEEE Transactions on Neural Networks* **17**, 820–824 (2006).

25. Gandhi, M., Tiño, P. & Jaeger, H. Theory of input driven dynamical systems. In *European Symposium on Artificial Neural Networks, Computational Intelligence and Machine Learning*, 25–27 (2012).
26. Lukoševicius, M. & Jaeger, H. Overview of reservoir recipes. *Jacobs University Bremen, Technical Reports* (2007).
27. Mackey, M. C. & Glass, L. Oscillation and chaos in physiological control systems. *Science* **197**, 287–289 (1977).
28. Hübner, U., Abraham, N. & Weiss, C. Dimensions and entropies of chaotic intensity pulsations in a single-mode far-infrared NH_3 laser. *Physical Review A* **40**, 6354 (1989).
29. Hammami, N. & Bedda, M. Improved tree model for arabic speech recognition. In *Computer Science and Information Technology (ICCSIT), 2010 3rd IEEE International Conference on*, vol. 5, 521–526 (IEEE, 2010).
30. Holzmann, G. & Hauser, H. Echo state networks with filter neurons and a delay&sum readout. *Neural Networks* **23**, 244–256 (2010).
31. Crucitti, P., Latora, V., Marchiori, M. & Rapisarda, A. Efficiency of scale-free networks: error and attack tolerance. *Physica A: Statistical Mechanics and its Applications* **320**, 622–642 (2003).
32. Albert, R., Jeong, H. & Barabási, A.-L. Error and attack tolerance of complex networks. *Nature* **406**, 378–382 (2000).

33. Castellano, C. & Pastor-Satorras, R. Thresholds for epidemic spreading in networks. *Physical Review Letters* **105**, 218701 (2010).
34. Pastor-Satorras, R. & Vespignani, A. Epidemic spreading in scale-free networks. *Physical Review Letters* **86**, 3200 (2001).
35. Vespignani, A. Complex networks: The fragility of interdependency. *Nature* **464**, 984–985 (2010).
36. Liu, Y.-Y., Slotine, J.-J. & Barabási, A.-L. Controllability of complex networks. *Nature* **473**, 167–173 (2011).
37. Barabási, A.-L. *et al.* Scale-free networks: a decade and beyond. *Science* **325**, 412 (2009).
38. Liebald, B. *Exploration of effects of different network topologies on the ESN signal crosscorrelation matrix spectrum*. Ph.D. thesis, University Bremen (2004).
39. Cui, H., Liu, X. & Li, L. The architecture of dynamic reservoir in the echo state network. *Chaos: An Interdisciplinary Journal of Nonlinear Science* **22**, 033127 (2012).
40. Jaeger, H. *Short term memory in echo state networks* (GMD-Forschungszentrum Informationstechnik, 2001).
41. Lukoševičius, M. & Jaeger, H. Reservoir computing approaches to recurrent neural network training. *Computer Science Review* **3**, 127–149 (2009).

42. Jaeger, H. Reservoir riddles: Suggestions for echo state network research. In *Proceedings. 2005 IEEE International Joint Conference on Neural Networks, 2005.*, vol. 3, 1460–1462 (IEEE, 2005).
43. Jaeger, H., Lukosevicius, M., Popovici, D. & Siewert, U. Optimization and applications of echo state networks with leaky-integrator neurons. *Neural Networks* **20**, 335–352 (2007).
44. Huebner, U., Klische, W., Abraham, N. & Weiss, C. On problems encountered with dimension calculations. In *Measures of Complexity and Chaos*, 133–136 (Springer, 1989).
45. Lichman, M. UCI machine learning repository (2013). URL <http://archive.ics.uci.edu/ml>.
46. Cameron, T. & Griffin, J. An alternating frequency/time domain method for calculating the steady-state response of nonlinear dynamic systems. *Journal of Applied Mechanics* **56**, 149–154 (1989).
47. Brincker, R., Zhang, L. & Andersen, P. Modal identification of output-only systems using frequency domain decomposition. *Smart Materials and Structures* **10**, 441 (2001).
48. Wei, W. W.-S. *Time series analysis* (Addison-Wesley publ Reading, 1994).
49. Soliman, S. S. & Srinath, M. D. Continuous and discrete signals and systems. *Englewood Cliffs, NJ, Prentice Hall, 1990, 523 p.* **1** (1990).
50. Elliott, D. F. *Handbook of digital signal processing: engineering applications* (Academic Press, 2013).

51. Deco, G. & Schuermann, B. *Information dynamics: foundations and applications* (Springer Science, 2012).
52. Mermelstein, P. Distance measures for speech recognition, psychological and instrumental. *Pattern Recognition and Artificial Intelligence* **116**, 374–388 (1976).